

Antenna Coupling and Near-Field Sampling in Plane-Polar Coordinates

Arthur D. Yaghjian, *Senior Member, IEEE*

Abstract—A probe-corrected vector transmission formula and a rigorous sampling-reconstruction theorem for near-field antenna measurements in plane-polar coordinates are derived from three fundamental theorems of antenna theory: the mutual coupling function between two antennas satisfies the homogeneous wave equation; a receiving antenna can be represented as a differentiator of the incident field; and the mutual coupling function is virtually bandlimited. The rigorous sampling equations are applied to compute the far fields of a circular-aperture antenna sampled in the near field at half-wavelength radial spacing.

I. INTRODUCTION

DURING the past decade a substantial amount of work has been done and a number of fine articles have been written on the subject of planar near-field antenna measurements in polar coordinates [1]–[8]. However, there appears missing from the published literature a rigorous sampling theorem with uniform radial spacing for plane-polar measurements and computations. The rigorous sampling theorem with $\lambda/2$ data point spacing for plane-rectangular scanning does not apply to the radial eigenfunction expansions of plane-polar scanning. Also, there appears absent from the literature a detailed formulation of probe-corrected plane-polar scanning from first principles directly in polar coordinates. The approach in the past has been to base the plane-polar derivations on the formulas from plane-rectangular near-field scanning. Thus, it is the purpose of this paper to derive, directly in plane-polar coordinates, rigorous formulas for near-field antenna coupling and uniform $\lambda/2$ radial sampling.

The derivations are based on three fundamental theorems of antenna theory. One, the mutual coupling function between two antennas, which translate with respect to each other without rotation, satisfies the homogeneous wave equation when multiple interactions are neglected. Two, the output of a receiving antenna can be expressed as a linear differential operator converting the incident field and its spatial derivatives at a single point in space to an output voltage. Three, the mutual coupling function expanded in plane-polar as well as rectangular eigenfunctions is virtually bandlimited by the free-space propagation constant if the antennas remain outside their reactive zones.

Manuscript received May 17, 1991; revised December 10, 1991.

The author is with the Electromagnetics Directorate, Rome Laboratory/ERCT, Hanscom AFB, MA 01731.
IEEE Log Number 9106606.

The first theorem is applied to derive directly a vector plane-polar transmission formula and related expressions for the fields of the test antenna. The second is applied to determine the effect on the vector output of the probe of rotating the probe antenna with respect to the test antenna, or equivalently, the effect on plane-polar data of rotating the test antenna without co-rotating the probe. The third theorem is applied to derive a rigorous sampling-reconstruction theorem for straightforward evaluation of the plane-polar representation coefficients and fields of the test antenna using $\lambda/2$ radial data-point spacing.

Comparisons are made with previous plane-polar expressions, and numerical results are presented for a hypothetical uniformly illuminated circular-aperture test antenna. Finally, computer run times are discussed for different methods of processing the plane-polar near-field data.

II. DERIVATION OF TRANSMISSION FORMULA FOR PLANE-POLAR SCANNING

Consider a receiving probe antenna scanning in free space on a plane in front of a transmitting test antenna, as shown in Fig. 1. The xyz axes with origin O are fixed in the test antenna, and the reference origin O_p fixed in the probe antenna moves in the plane $z = z_0$ with polar coordinates (ρ, ϕ) measured from the origin O and the x -axis. Both the probe and test antennas respond linearly with single-mode feeds at frequencies ω within their usable bandwidths. (Time dependence of $\exp(-i\omega t)$ with $\omega > 0$ is used throughout.) The input modal coefficient for the test antenna at the reference surface S_0 is given by a_0 , and the output modal coefficient for the probe antenna at the reference surface S_p is given by b_p .

A. Expansion of the Probe Response in Plane-Polar Coordinates

In order to determine the complete transmitting characteristics of the test antenna, the output of the probe should be recorded in two independent polarizations; namely at orientation $\psi = 0^\circ$ and $\psi = 90^\circ$ about the z_p -axis through O_p parallel to z . In each of these orientations it is assumed that the probe translates without rotation in the scan plane. That is, if the scanning is performed by rotating the test antenna, the probe antenna is co-rotated to keep the relative orientation of the probe and test antennas the same. In Section III the formulation is generalized to allow plane-polar scanning without co-rotation.

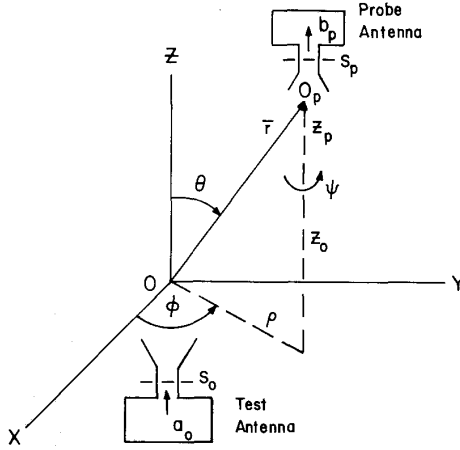


Fig. 1. The receiving probe that scans in polar coordinates on the plane $z = z_0$.

It proves convenient to define the vector response of the probe for arbitrary z -position as a vector sum of the scalar responses in the two orientations:

$$\bar{b}_t(\rho, \phi, z) = b_p(\psi = 0^\circ) \hat{x} + b_p(\psi = 90^\circ) \hat{y}. \quad (1)$$

If the probe in the $\psi = 0^\circ$ orientation were an electric or magnetic dipole in the x -direction, \bar{b}_t would be proportional to the electric or magnetic field, respectively, transverse to the z -direction.

In [9], and the Appendix of this paper, it is proven that the mutual coupling function between two antennas, that translate with respect to each other without rotation, satisfies the homogeneous scalar wave equation, provided multiple interactions between the two antennas are neglected and the two antennas remain a large enough distance apart to allow an infinite free-space plane between them (i.e., the antennas do not "encroach" upon each other). Consequently, under these assumptions, the vector response of the probe defined in (1) satisfies

$$\nabla^2 \bar{b}_t + k^2 \bar{b}_t = 0. \quad (2)$$

Note that the definition (1) of the vector response \bar{b}_t of the probe depends on the chosen orientation of the probe at $\psi = 0^\circ$ with respect to the test antenna. Except for certain probe antennas discussed in Section III, the vector response of the probe will change if the $\psi = 0^\circ$ reference orientation and the xy axes are rotated the same amount about the z_p and z axes, respectively, holding fixed the test antenna. Also $\hat{u} \cdot \bar{b}_t$ does not, in general, equal the scalar output of the probe when the $\psi = 0^\circ$ reference orientation is aligned with a transverse unit vector \hat{u} other than \hat{x} or \hat{y} . Nonetheless, once the orientation of the probe at $\psi = 0^\circ$ and the xy axes are fixed with respect to the test antenna, \bar{b}_t is a vector that can be written in any desired coordinate system, and which satisfies the wave equation (2) in an arbitrary coordinate system.

Each of the rectangular components of the wave equation (2) separates in plane-polar, circular cylindrical coordinates to yield the complete set of free-space modes [10].

$$J_n(K\rho) e^{i\gamma z} e^{in\phi}, \quad \begin{cases} 0 \leq K < \infty \\ n = 0, \pm 1, \pm 2 \dots \end{cases} \\ \gamma = (k^2 - K^2)^{1/2} \quad (3)$$

with γ chosen positive real or positive imaginary in the forward z -hemisphere, depending on whether K is less than or greater than the free-space wavenumber $k = \omega/c = 2\pi/\lambda$ (c being the speed of light and λ the wavelength). Expanding $\bar{b}_t(\rho, \phi, z)$ in these circular cylindrical modes, one obtains in the forward free-space hemisphere

$$\bar{b}_t(\rho, \phi, z) = \sum_{n=-\infty}^{\infty} e^{in\phi} \int_0^\infty \bar{D}_n(K) J_n(K\rho) e^{i\gamma z} K dK \quad (4)$$

in which the $\bar{D}_n(K)$ are unknown modal coefficients of the response of the probe to the test antenna. Using the orthogonality relation for the circular cylindrical modes:

$$\int_0^\infty \int_0^{2\pi} J_{n'}(K'\rho) J_n(K\rho) e^{i(n-n')\phi} \rho d\phi d\rho = \frac{2\pi \delta_{nn'} \delta(K-K')}{K} \quad (5)$$

we can solve for the $\bar{D}_n(K)$ in terms of the measured data $\bar{b}_t(\rho, \phi, z_0)$ on the plane $z = z_0$; specifically

$$\bar{D}_n(K) = \frac{e^{-i\gamma z_0}}{2\pi} \int_0^\infty \int_0^{2\pi} \bar{b}_t(\rho, \phi, z_0) J_n(K\rho) \cdot e^{-in\phi} \rho d\phi d\rho. \quad (6)$$

Note that once the $\bar{D}_n(K)$ are found by integrating in (6) over the measured data on the z_0 plane, the vector response for any other z -plane can be found by integrating and summing $\bar{D}_n(K)$ in (4). Next $\bar{D}_n(K)$ will be related to the far fields of the probe and test antennas.

B. Fields and Spectrum of the Test Antenna

When the probe antenna is withdrawn to the far field of the test antenna, the cylindrical coordinates ρ and z approach infinity and the integral in (4) can be evaluated asymptotically by the method of stationary phase to give

$$\bar{b}_t(r, \phi, \theta) \xrightarrow{r \rightarrow \infty} -ik \cos \theta \frac{e^{ikr}}{r} \sum_{n=-\infty}^{\infty} (-i)^n \cdot \bar{D}_n(k \sin \theta) e^{in\phi}. \quad (7)$$

In the far-field expression (7), it is more convenient to use the spherical coordinates (r, ϕ, θ) than the cylindrical coordinates (ρ, ϕ, z) ; see Fig. 1. The response b_p of the probe in the far field is proportional to the scalar product of the far fields of the test antenna and the probe antenna. Specifically [9],

$$b_p(\psi = 0) \xrightarrow{r \rightarrow \infty} 2\pi i \frac{a_0 C_p}{k} \bar{f}_p^0(-\hat{r}) \cdot \bar{f}(\hat{r}) \frac{e^{ikr}}{r} \quad (8a)$$

$$b_p(\psi = 90^\circ) \xrightarrow{r \rightarrow \infty} 2\pi i \frac{a_0 C_p}{k} \bar{f}_p^{90}(-\hat{r}) \cdot \bar{f}(\hat{r}) \frac{e^{ikr}}{r} \quad (8b)$$

where $\bar{f}(\hat{r})$ and $\bar{f}_p^{0,90}(-\hat{r})$ are the complex far-field patterns defined in terms of the far electric fields of the test and probe antennas when each is radiating separately in free space with excitations a_0 and a_p , respectively:

$$\bar{f}(\hat{r}) \equiv \frac{re^{-ikr}}{a_0} \bar{E}(\bar{r})_{r \rightarrow \infty} \quad (9a)$$

$$\bar{f}_p^{0,90}(\hat{r}) \equiv \frac{re^{-ikr}}{a_p} \bar{E}_p^{0,90}(\bar{r})_{r \rightarrow \infty}. \quad (9b)$$

(If the probe antenna is nonreciprocal, one should replace the far field of the probe with the far field of the "adjoint" probe or the complex receiving pattern of the probe antenna. The minus signs are required in (8) on the \hat{r} in the probe's far-field patterns because all vectors in (8) are referenced to the coordinate system fixed in the test antenna; see Fig. 1. This is common practice in antenna coupling theory [11].) The constant C_p is defined as

$$C_p = [(1 - \Gamma_L \Gamma_0) \eta_0 Z_0]^{-1} \quad (10)$$

where η_0 is the characteristic admittance of the single propagating mode in the feed to the probe antenna, Z_0 is the impedance of free space, and Γ_0 and Γ_L are the reflection coefficients of the probe antenna and its passive termination, respectively, when the probe is receiving.

Substituting (8) into (1) to get the vector response of the probe as $r \rightarrow \infty$; then inserting this far-field vector response into the left side of (7) gives

$$\bar{\bar{R}}_p \cdot \bar{f}(\hat{r}) = -ik \cos \theta \sum_{n=-\infty}^{\infty} (-i)^n \cdot \bar{D}_n(k \sin \theta) e^{in\phi} \quad (11)$$

where $\bar{\bar{R}}_p$ is shorthand dyadic notation for the complete receiving characteristics of the probe antenna in both its orientations. It is given explicitly in terms of the probe's far-field patterns, which are assumed to have been determined through measurements or computations:

$$\bar{\bar{R}}_p = \frac{2\pi ia_0 C_p}{k} [\hat{x} \bar{f}_p^{0,90}(-\hat{r}) + \hat{y} \bar{f}_p^{90,0}(-\hat{r})]. \quad (12)$$

Defining the inverse of $\bar{\bar{R}}_p$ by

$$\bar{\bar{R}}_p^{-1} \cdot \bar{\bar{R}}_p = \hat{\phi} \hat{\phi} + \hat{\theta} \hat{\theta} \quad (13a)$$

or, specifically

$$\bar{\bar{R}}_p^{-1} = \frac{k}{2\pi ia_0 C_p} \hat{r} \times (\bar{f}_p^{90,0} \hat{x} - \bar{f}_p^{0,90} \hat{y}) / (f_{p\phi}^0 f_{p\theta}^{90} - f_{p\phi}^{90} f_{p\theta}^0) \quad (13b)$$

allows the complex vector far-field pattern of the test antenna to be written from (11) as

$$\bar{f}(\theta, \phi) = -ik \cos \theta \bar{\bar{R}}_p^{-1} \cdot \sum_{n=-\infty}^{\infty} (-i)^n \bar{D}_n(k \sin \theta) e^{in\phi}. \quad (14)$$

The far-field function (spectrum) can be found from $\bar{D}_n(K)$ for all values of the transverse wave parameter K , by writing $k \sin \theta$ in (14) as K , $k \cos \theta$ as γ , and ϕ as α to get

$$\bar{f}(K, \alpha) = -i\gamma \bar{\bar{R}}_p^{-1} \cdot \sum_{n=-\infty}^{\infty} (-i)^n \bar{D}_n(K) e^{in\alpha}. \quad (15)$$

The complete vectorial spectrum $\bar{f}(K, \alpha)$ can also be expressed in x and y components of rectangular wavenumbers k_x and k_y through applying the transformations

$$K = \sqrt{k_x^2 + k_y^2} \quad (16a)$$

$$\alpha = \tan^{-1} k_y / k_x \quad (16b)$$

to recast (15) in the form

$$\bar{f}(k_x, k_y) = -i\gamma \bar{\bar{R}}_p^{-1} \cdot \sum_{n=-\infty}^{\infty} (-i)^n \bar{D}_n(\sqrt{k_x^2 + k_y^2}) \cdot e^{in \tan^{-1} k_y / k_x}, \quad \gamma = (k^2 - k_x^2 - k_y^2)^{1/2} \quad (17)$$

which agrees with the transmission formula derived by Stubenrauch [2] from the plane-rectangular transmission equation [11].

The electric and magnetic fields of the test antenna anywhere in its free-space forward z -hemisphere are determined from the two-dimensional Fourier transforms of the complete spectrum [11]:

$$\bar{E}(x, y, z) = \frac{ia_0}{2\pi} \int_{-\infty}^{\infty} \int_{-\infty}^{\infty} \frac{\bar{f}(k_x, k_y)}{\gamma} \cdot e^{i\gamma z} e^{ik_x x} e^{ik_y y} dk_x dk_y \quad (18a)$$

$$\bar{H}(x, y, z) = \frac{ia_0}{2\pi Z_0} \int_{-\infty}^{\infty} \int_{-\infty}^{\infty} \frac{\hat{k} \times \bar{f}(k_x, k_y)}{\gamma} \cdot e^{i\gamma z} e^{ik_x x} e^{ik_y y} dk_x dk_y, \quad \bar{k} = k_x \hat{x} + k_y \hat{y} + \gamma \hat{z} \quad (18b)$$

or in polar coordinates

$$\bar{E}(\rho, \phi, z) = \frac{ia_0}{2\pi} \int_0^\infty \int_0^{2\pi} \frac{\bar{f}(K, \alpha)}{\gamma} \cdot e^{i\gamma z} e^{iK\rho \cos(\phi-\alpha)} K d\alpha dK \quad (19a)$$

$$\bar{H}(\rho, \phi, z) = \frac{ia_0}{2\pi Z_0} \int_0^\infty \int_0^{2\pi} \frac{\hat{k} \times \bar{f}(K, \alpha)}{\gamma} \cdot e^{i\gamma z} e^{iK\rho \cos(\phi-\alpha)} K d\alpha dK. \quad (19b)$$

One could, of course, substitute $\bar{f}(K, \alpha)$ from (15) into (19) and express the α integration as a Bessel function to recast (19) in terms of circular cylindrical modes of (3). Also, taking the inverse transform of (18a) or (18b) determines the usual plane-wave formula for the far electric field in terms of the near electric or magnetic field. For example, the inverse transform of (18a) gives

$$\bar{f}(\theta, \phi) = \frac{-ik \cos \theta}{2\pi a_0} e^{-ikz \cos \theta} \int_0^\infty \int_0^{2\pi} \bar{E}(\rho', \phi', z) \cdot e^{-ik\rho' \sin \theta \cos(\phi-\phi')} \rho' d\phi' d\rho' \quad (20)$$

after the (x, y) integration coordinates are written in the polar coordinates (ρ', ϕ') by means of $x = \rho' \cos \phi'$, $y = \rho' \sin \phi'$, and $\rho' d\phi' d\rho'$ replacing $dx dy$; and (k_x, k_y) are changed to the spherical coordinates (θ, ϕ) by means of $k_x = k \sin \theta \cos \phi$ and $k_y = k \sin \theta \sin \phi$.

In summary, the plane-polar modal coefficients $\bar{D}_n(K)$ are found from the integrals of the measured probe output $\bar{b}_i(\rho, \phi, z_0)$ in (6). The complex vectorial far-field pattern or complete transmitting spectrum \bar{f} of the test antenna is found from the summation of the modal coefficients $\bar{D}_n(K)$ in (14) or (15). And the electric and magnetic fields of the test antenna can be found on any other free-space plane of its forward hemisphere by integrating its spectrum in (18) or (19). In section 4 a plane-polar sampling-reconstruction theorem is derived for accurately computing the modal coefficients $\bar{D}_n(K)$ from the integrals of the measured data in (6). First, however, let us consider the possibility, mentioned above, of plane-polar scanning by rotating the test antenna but without co-rotating the probe antenna.

III. PLANE-POLAR SCANNING WITHOUT CO-ROTATION

Recall that the vector response (\bar{b}_i) of the probe satisfies the wave equation (2), provided the probe translates without rotation with respect to the test antenna. Thus, in general, if the plane-polar data is taken by rotating the test antenna and moving the probe on a linear track without co-rotating the probe about its z_p -axis to compensate for the rotation of the test antenna, (2) and the analysis of Section II does not apply. Fortunately, if the complex receiving pattern of the probe antenna has only first-order azimuthal dependence, the vector response of the probe is unchanged by rotation about its z_p -axis [2], [12]. This result can be proven directly and conveniently from the linear differential operator representation of a receiving antenna as derived in [13].

Specifically, it is proven in [13] that the vector response $\bar{b}_i(\bar{r})$ of an arbitrary receiving antenna (probe) can be expressed as a linear operator, involving the complex receiving pattern of the probe, differentiating the incident electric and magnetic fields at a point \bar{r} to which the receiving pattern is referenced. That is, the vector probe response can be written

$$\bar{b}_i(\bar{r}) = \bar{\mathcal{L}}_E(\bar{r}) \cdot \bar{E}(\bar{r}) + Z_0 \bar{\mathcal{L}}_H(\bar{r}) \cdot \bar{H}(\bar{r}) \quad (21)$$

where $\bar{\mathcal{L}}_E(\bar{r})$ and $\bar{\mathcal{L}}_H(\bar{r})$ are dyadic differential operators defined in terms of the receiving pattern of the probe antenna (or the far-field pattern of reciprocal probes).

Initially, let \bar{r} in (21) be the xyz coordinates of the fields of the test antenna in Fig. 1. Then rotate the probe an angle ψ' about the z_p -axis so that the probe is now aligned with respect to $x' y' z$ axes, as it was with respect to the xyz axes before rotation. Then the new vector response of the probe defined by

$$\bar{b}'_i(x', y', z) \equiv b_p(\psi = \psi') \hat{x}' + b_p(\psi = \psi' + 90^\circ) \hat{y}' \quad (22)$$

can be written from (21) as

$$\bar{b}'_i(x', y', z) = \bar{\mathcal{L}}'_E(x', y', z) \cdot \bar{E}'(x', y', z) + Z_0 \bar{\mathcal{L}}'_H(x', y', z) \cdot \bar{H}'(x', y', z). \quad (23a)$$

Since the electric and magnetic fields are simply vectors at a point in space, they are the same whether referred to the $x' y' z$ or xyz coordinate system. Thus $\bar{E}'(x', y', z)$ and $\bar{H}'(x', y', z)$ can be replaced by $\bar{E}(x, y, z)$ and $\bar{H}(x, y, z)$, respectively, so that (23a) may be rewritten as

$$\bar{b}'_i(x', y', z) = \bar{\mathcal{L}}'_E(x', y', z) \cdot \bar{E}(x, y, z) + Z_0 \bar{\mathcal{L}}'_H(x', y', z) \cdot \bar{H}(x, y, z). \quad (23b)$$

For an arbitrary probe $\bar{\mathcal{L}}'_E(x', y', z)$ and $\bar{\mathcal{L}}'_H(x', y', z)$ are not equal to $\bar{\mathcal{L}}_E(x, y, z)$ and $\bar{\mathcal{L}}_H(x, y, z)$, respectively, so that $\bar{b}'_i(x', y', z)$ will not, in general, equal the original vector response $\bar{b}_i(x, y, z)$, i.e., the vector response of the probe with $\psi' = 0^\circ$. However, for probes that have receiving patterns with only first-order azimuthal dependence about their z_p -axis in Fig. 1, such as the probes used for spherical near-field scanning [14], [15], it can be proven [13] that

$$\bar{\mathcal{L}}'_E(x', y', z) = \bar{\mathcal{L}}_E(x, y, z) \quad (24a)$$

$$\bar{\mathcal{L}}'_H(x', y', z) = \bar{\mathcal{L}}_H(x, y, z). \quad (24b)$$

Consequently, the vector response in (22) for these probes does not change with rotation angle ψ' (when the unit vectors \hat{x}' and \hat{y}' are written in terms of the original unit vectors \hat{x} and \hat{y}), and the plane-polar analysis of Section II remains valid.

Electric and magnetic dipole probes that measure the transverse electric and magnetic fields are special cases of azimuthally first-order probes. Also, to a good approximation, open-ended waveguides behave as azimuthally first-order probes over their recommended usable bandwidths [13], [16].

A. An Alternative Analysis of Rotating Probes

A simple alternative method to arrive at the results of the previous section is to begin with the definition in (22) of the vector response of the probe rotated by the angle ψ' . The rotated (\hat{x}', \hat{y}') unit vectors in (22) are related to the original (\hat{x}, \hat{y}) unit vectors of Fig. 1 by the simple transformations

$$\hat{x}' = \hat{x} \cos \psi' + \hat{y} \sin \psi' \quad (25a)$$

$$\hat{y}' = -\hat{x} \sin \psi' + \hat{y} \cos \psi' \quad (25b)$$

so that (22) becomes

$$\bar{b}'_i = [b_p(\psi') \cos \psi' - b_p(\psi' + 90^\circ) \sin \psi'] \hat{x} + [b_p(\psi') \sin \psi' + b_p(\psi' + 90^\circ) \cos \psi'] \hat{y}. \quad (26)$$

Expanding the scalar response $b_p(\psi')$ in a Fourier series, we have

$$b_p(\psi') = \sum_{n=0}^{\infty} [a_n \sin n\psi' + b_n \cos n\psi'] \quad (27a)$$

$$b_p(\psi' + 90^\circ) = \sum_{n=0}^{\infty} [a_n \sin n(\psi' + 90^\circ) + b_n \cos n(\psi' + 90^\circ)]. \quad (27b)$$

If all the Fourier coefficients, a_n and b_n , are zero except for $n = 1$, (27) reduces to

$$b_p(\psi') = a_1 \sin \psi' + b_1 \cos \psi' \quad (28a)$$

$$b_p(\psi' + 90^\circ) = a_1 \cos \psi' - b_1 \sin \psi'. \quad (28b)$$

Substitution of (28) into (26) yields a vector probe response

$$\bar{b}_i' = b_1 \hat{x} + a_1 \hat{y} \quad (29)$$

that is independent of ψ' .

Q.E.D.

This alternative method of determining the effect of rotating the probe is appealing because of its simplicity. However, it does not provide a theoretical framework for proving that the first-order scalar responses of the probe assumed in (28) will indeed be the responses exhibited by probes whose complex receiving patterns have only first-order azimuthal dependence, or by reciprocal probes that radiate only first-order azimuthally dependent fields. To prove this result one can rely on more detailed analyses, such as the theory of spherical scanning [12], [15] or the linear operator method [13] used above in Section III.

IV. RIGOROUS SAMPLING THEOREM IN PLANE-POLAR COORDINATES

It is possible to determine the sample spacing of the measured data $\bar{b}_i(\rho, \phi, z_0)$ in ρ and ϕ required to accurately compute the modal coefficients $\bar{D}_n(K)$ (and thus the fields radiated by the test antenna) from the plane-polar integral of (6) converted to a summation. Specifically, an angular sampling theorem (34) is derived that allows the probe to sample points in the near field at uniform angular spacings that may, if desired, grow larger with decreasing values of the radial scanning coordinate ρ . More importantly, a rigorous sampling theorem (39) and reconstruction formula (44) are derived that allow, for the first time, the fields of the test antenna to be computed accurately from measured data taken at uniform $\lambda/2$ spacing in the radial direction.

To derive these plane-polar sampling theorems, begin by rewriting (6) as

$$\bar{D}_n(K) e^{i\gamma z_0} = \int_0^{\rho_0} \bar{b}_n(\rho, z_0) J_n(K\rho) \rho d\rho \quad (30)$$

$$\bar{b}_n(\rho, z_0) = \frac{1}{2\pi} \int_0^{2\pi} \bar{b}_i(\rho, \phi, z_0) e^{-in\phi} d\phi. \quad (31)$$

(The infinite upper limit of integration in (6) has been replaced in (30) by the finite radius ρ_0 of the scan plane.)

A. Sampling in ϕ

Because $\gamma = (k^2 - K^2)^{1/2}$ becomes positive imaginary for $K > k$, the exponential on the left-hand side of (30) becomes extremely small for z_0 greater than about a wavelength and K slightly larger than k . Thus, the left side of (30) is negligible for $K > k^+$ (k^+ denoting a value a small percent larger than k) provided $\bar{D}_n(K)$ does not grow extremely large for $K > k$. Furthermore, Poynting's theorem applied to the fields of the test antenna shows that $\bar{D}_n(K)$ will not become extremely large for $K > k$ unless

reactive fields extend well beyond a wavelength from the physical test antenna [17]. In other words, the left-hand side of (30) is effectively zero for $K > k^+$, and z_0 outside the reactive region of the test antenna, or more precisely, for the test and probe antennas separated far enough so that their reactive fields do not interact. Consequently, $\bar{b}_n(\rho, z_0)$ can be written as a *finite* integral over $\bar{D}_n(K)$ by applying the orthogonality of the Bessel functions:

$$\bar{b}_n(\rho, z_0) = \int_0^{k^+} \bar{D}_n(K) J_n(K\rho) e^{i\gamma z_0} K dK. \quad (32)$$

(Alternatively, (32) can be gotten by inserting \bar{b}_i from (4) into (31).)

The Bessel functions $J_n(x)$ grow extremely small, very rapidly for $|n| > x$. Thus, the integral in (32) and $\bar{b}_n(\rho, z_0)$ is virtually zero for $|n| > k^+\rho$, again provided the separation distance z_0 is large enough for the antennas to be outside their reactive zones. Once ρ is large enough to intersect the minimum sphere circumscribing the test antenna, the theory of spherical scanning [15] tells us that $\bar{b}_n(\rho, z_0)$ is practically zero for $|n| > k^+a \sin \theta$. Thus, $\bar{b}_n(\rho, z_0)$ is bandlimited to the integer N closest to the smaller of

$$[k^+(\rho + \lambda), k^+(a \sin \theta + \lambda)]. \quad (33)$$

(The λ is included in (33) to cover the possibility of the value of ρ or $a \sin \theta$ being much less than a wavelength. The values of N given in (33) vary with ρ . We can, of course, set N equal to a constant larger than the values given in (33), namely $N = k^+(a + \lambda)$.)

Under the bandlimit of (33), the sampling theorem for Fourier series [18] can be applied to convert the ϕ -integration in (31) to the summation

$$\bar{b}_n(\rho, z_0) = \frac{\Delta\phi}{2\pi} \sum_{l=0}^M \bar{b}_i(\rho, l\Delta\phi, z_0) e^{-inl\Delta\phi}, \quad |n| \leq N$$

$$\Delta\phi = \frac{2\pi}{M+1}, \quad M \geq 2N. \quad (34)$$

The angular sampling theorem (34) is very similar to the corresponding azimuthal angular sampling theorems that have been derived for spherical and cylindrical scanning [15], [19], and for plane-polar scanning by Bucci *et al.* [8].

B. Sampling in ρ

After $\bar{b}_n(\rho, z_0)$ is evaluated from the summation in (34) over the azimuthally sampled vector response of the probe, $\bar{D}_n(K)$ is evaluated from the radial integral in (30). A rigorous sampling theorem is derived for this radial integral in (30), by using the result of the previous section that $\bar{D}_n(K) e^{i\gamma z_0}$ is effectively zero for $K > k^+$, and z_0 large enough that the reactive zones of the antennas do not appreciably interact. Assuming this is the case, $\bar{D}_n(K) e^{i\gamma z_0}$ can be expanded in a complete Fourier-Bessel series [20]

$$\bar{D}_n(K) e^{i\gamma z_0} = \sum_{m=1}^{\infty} \bar{C}_{nm} J_n(\alpha_{nm} K / k^+), \quad 0 < K < k^+ \quad (35)$$

where $J_n(\alpha_{nm}) = 0$, i.e., α_{nm} are the zeros of the n th order Bessel function. (The key to a rigorous sampling theorem in

the radial coordinate is to expand the plane-polar modal coefficients in a Fourier-Bessel series (35), *not the measured data.*)

Applying the orthogonality relation

$$\int_0^{k^+} J_n(\alpha_{nm} K/k^+) J_n(\alpha_{nm} K/k^+) K dK = \frac{\delta_{mm'}}{2} [k^+ J'_n(\alpha_{nm})]^2 \quad (36)$$

to (35), the unknown coefficients \bar{C}_{nm} emerge as

$$\bar{C}_{nm} = \frac{2}{[k^+ J'_n(\alpha_{nm})]^2} \int_0^{k^+} \bar{D}_n(K) \cdot e^{i\gamma z_0} J_n(\alpha_{nm} K/k^+) K dK. \quad (37)$$

Comparing (37) with (32), one sees that \bar{C}_{nm} is related to $\bar{b}_n(\rho, z_0)$ by

$$\bar{C}_{nm} = \frac{2}{[k^+ J'_n(\alpha_{nm})]^2} \bar{b}_n(\alpha_{nm}/k^+, z_0). \quad (38)$$

Substitution of \bar{C}_{nm} from (38) into (35) gives us a rigorous sampling theorem (with nonuniform spacing) for the radial integration in plane-polar scanning:

$$\bar{D}_n(K) = \frac{2e^{-i\gamma z_0}}{k^{+2}} \sum_{m=1}^{\infty} \frac{\bar{b}_n(\rho_{nm}, z_0)}{[J'_n(\alpha_{nm})]^2} J_n(K\rho_{nm}), \quad 0 < K < k^+, \rho_{nm} \equiv \alpha_{nm}/k^+. \quad (39)$$

In practice, the infinite limit on the summation in (39) is replaced by M determined from the radius of the scan plane, i.e., M is given by

$$\rho_{nM} = \rho_0. \quad (40)$$

(The effect of truncating the scan plane is discussed in Section V.) Also, one can, of course, choose smaller sampling increments by replacing k^+ in (39) by any value larger than k^+ . Sampling equations similar to (39) were derived by Barakat [21] for $n = 0$, and by Stark [22] for arbitrary n .

1) Reconstruction of Data Measured at $\lambda/2$ Radial Spacing: The zeros of the Bessel functions are separated by values approximately equal to π . Thus, the data $\bar{b}_n(\rho_{nm}, z_0)$ in the radial sampling summation of (39) is required at ρ_{nm} separated by about $\lambda/2$. Unfortunately, the values of ρ_{nm} are not the same for each n . This means that measured data at equal spacings in ρ cannot be used directly in the summation of (39) to evaluate the $\bar{D}_n(K)$. To allow use of measured data taken at equal radial spacings of $\pi/k^+ \approx \lambda/2$, a rigorous reconstruction formula can be derived to compute $\bar{b}_n(\rho_{nm}, z_0)$ in (39) at the required values of ρ_{nm} .

The derivation of the reconstruction formula begins by extending the measured data $\bar{b}_n(\rho, z_0)$ to negative values of ρ through the integral in (32). Since $J_n(-K\rho) = (-1)^n J_n(K\rho)$, (32) implies that

$$\bar{b}_n(-\rho, z_0) = (-1)^n \bar{b}_n(\rho, z_0). \quad (41)$$

Next expand this analytically continued data in a Fourier transform

$$\bar{b}_n(\rho, z_0) = \int_{-\infty}^{\infty} \bar{\beta}_n(s, z_0) e^{is\rho} ds \quad (42a)$$

$$\bar{\beta}_n(s, z_0) = \frac{1}{2\pi} \int_{-\infty}^{\infty} \bar{b}_n(\rho, z_0) e^{-is\rho} d\rho. \quad (42b)$$

Since $\bar{b}_n(\rho, z_0)$ is essentially measured data from $\rho = -\infty$ to $\rho = +\infty$, it has the same spacial frequency content as plane-rectangular data over a rectangular near-field coordinate from $-\infty$ to $+\infty$. Namely, its spectrum $\bar{\beta}_n(s, z_0)$ is bandlimited to $|s| = k^+$, again assuming the test and probe antennas lie outside their reactive fields (typically $z_0 > \lambda$). Consequently, $\bar{\beta}_n(s, z_0)$ can be written as a Fourier series

$$\bar{\beta}_n(s, z_0) = \frac{\Delta\rho}{2\pi} \sum_{l=-L}^L \bar{b}_n(\rho_l, z_0) e^{-is\rho_l}, \quad 0 < |s| < k^+, \Delta\rho = \pi/k^+ \approx \lambda/2 \quad (43)$$

with L chosen so that ρ_l spans the scan plane from $-\rho_0$ to ρ_0 in increments of $\Delta\rho$, i.e., $L \approx \rho_0/\Delta\rho$.

Substituting (43) into (42a) (after changing the infinite limits of integration in (42a) to $\pm k^+$) and interchanging the summation and integration, one finds

$$\bar{b}_n(\rho, z_0) = \frac{\Delta\rho}{\pi} \sum_{l=-L}^L \bar{b}_n(\rho_l, z_0) \frac{\sin k^+(\rho - \rho_l)}{\rho - \rho_l} \quad (44)$$

where we have used the result

$$\int_{-k^+}^{k^+} e^{is(\rho - \rho_l)} ds = \frac{2 \sin k^+(\rho - \rho_l)}{\rho - \rho_l}. \quad (45)$$

The formula (44) reconstructs the data function $\bar{b}_n(\rho, z_0)$ for any value of ρ on the scan plane from the data $\bar{b}_n(\rho_l, z_0)$ measured at the discrete points ρ_l separated by the equal radial spacing $\Delta\rho = \pi/k^+ \approx \lambda/2$. In particular (44) can be used to compute $\bar{b}_n(\rho_{nm}, z_0)$ needed in the plane-polar radial sampling summation of (39). The combination of the reconstruction formula (44) and the radial sampling equation (39) produces a rigorous plane-polar sampling-reconstruction theorem for measured data equally spaced with $\lambda/2$ increments in the radial direction. It is emphasized that merely converting the integral in (30) to a summation over values of ρ separated by $\lambda/2$ does not constitute a rigorous sampling equation, nor does it yield an accurate approximation to the integral, as the numerical results of the next section demonstrate.

The crucial step that allows reconstruction of $\bar{b}_n(\rho, z_0)$ from its values at equally spaced increments is the analytic continuation (41) of $\bar{b}_n(\rho, z_0)$, by means of the integral in (32), to negative values of ρ . One could, of course, reconstruct the near-field measured data before doing the ϕ integration. However, this latter reconstruction involves both ρ and ϕ , and would take a prohibitive amount of computer time proportional to $(ka)^4$ rather than the $(ka)^3$ computer time required for reconstruction of the $\bar{b}_n(\rho_{nm}, z_0)$ from (44); see Section V-A.

V. NUMERICAL RESULTS

The reconstruction and sampling equations, (44) and (39), were applied to a hypothetical circular-aperture antenna with a radius a of 15 wavelengths, uniformly excited by a linearly polarized electric field E_0 in the x -direction. The probe was assumed to measure the x -component of the electric field on a scan plane $z_0 = 1.25a = 18.75\lambda$ in front of the circular-aperture test antenna. The radius ρ_0 of the scan plane equaled $8a$. See Fig. 2.

Because of the circular symmetry of this hypothetical antenna, all the modal coefficients $\bar{D}_n(K)$ are zero except for $n = 0$. This means that the far field of the test antenna, as determined by (14), is proportional to \bar{D}_0 alone, and that the reconstruction and sampling equations are applied for $n = 0$ only.

To obtain the measured data, sampled at radial increments of $\lambda/2$, to be inserted into the reconstruction formula (44), an efficient algorithm was used for computing the near fields of a uniform circular-aperture antenna [23]. With these near fields, the values of $\bar{b}_0(\rho_{0m}, z_0)$ at ρ_{0m} were reconstructed from (44). The zeros of the Bessel function were found from convenient formulas in Abramowitz and Stegun [24]. The $\bar{b}_0(\rho_{0m}, z_0)$ were then summed in the sampling equation (39) to compute $\bar{D}_0(K) = D_0(K)\hat{x}$. From (14) the far field in the yz plane can be given simply in terms of D_0 as

$$f(\theta) = -ik \cos \theta D_0(k \sin \theta). \quad (46)$$

Fig. 3 shows the far-field gain function versus angle θ from boresight of the circular test antenna determined from the computed values of $D_0(k \sin \theta)$ in (46). The gain function for this hypothetical antenna is also computed from the well-known exact far field [25] of the circular-aperture antenna

$$f(\theta)_{\text{exact}} = -ia \cos \theta \frac{J_1(ka \sin \theta)}{\sin \theta} \quad (47)$$

and shown by the solid line in Fig. 3. The agreement between the exact gain function and the gain function computed from the plane-polar reconstruction and sampling equations, (44) and (39), is good until θ gets close to the scan angle limit θ_0 (see Fig. 2). The percent error, defined as the positive difference between the exact and computed far fields divided by the envelope of the exact far field, is shown in Fig. 4. For the far-field pattern well away from θ_0 , the error is less than 1%.

Fig. 5 shows the far-field pattern obtained by summing the radial integral in (30) directly at equal sample point spacings of $\lambda/2$, i.e., without using the rigorous reconstruction and sampling equations (44) and (39). Visually, the comparison between the exact and computed far-field patterns in Fig. 5 shows decent agreement. However, Fig. 6 reveals that this nonrigorously computed far field is in error by more than 10% over much of its pattern, a tenfold degradation from the pattern computed in Fig. 3 from the rigorous reconstruction-sampling equations. For actual antennas, this large error may have a devastating effect on the computed cross polarization, and low sidelobes. Even when the sample spacing was re-

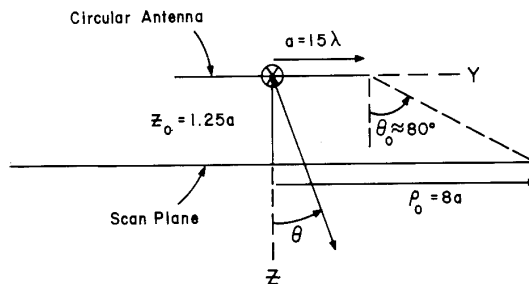


Fig. 2. Plane-polar scanning of a hypothetical circular-aperture test antenna.

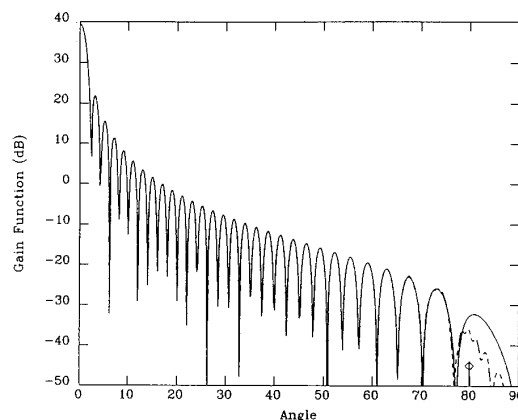


Fig. 3. Gain function of circular-aperture antenna; — exact, ---- computed from radial sampling-reconstruction theorem.

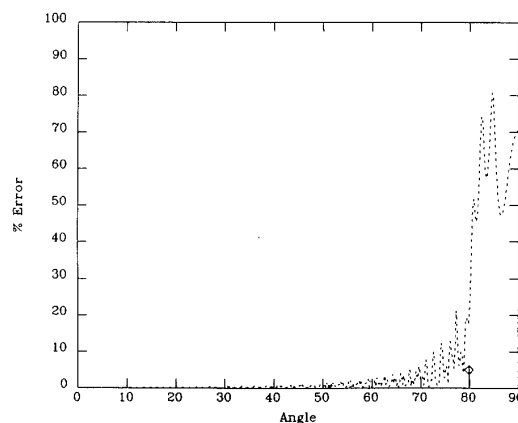


Fig. 4. Error between exact and computed far fields of Fig. 3.

duced to $\lambda/4$, the average error from 0° to 60° in using the direct sum remained greater than the average error in Fig. 4 using the rigorous reconstruction-sampling equations at $\lambda/2$ spacing.

In principle, the far fields computed from the reconstruction and sampling equations, (44) and (39), should contain errors hardly larger than the round off errors of the computer, because with a separation distance of $z_0 = 18.75\lambda$ the

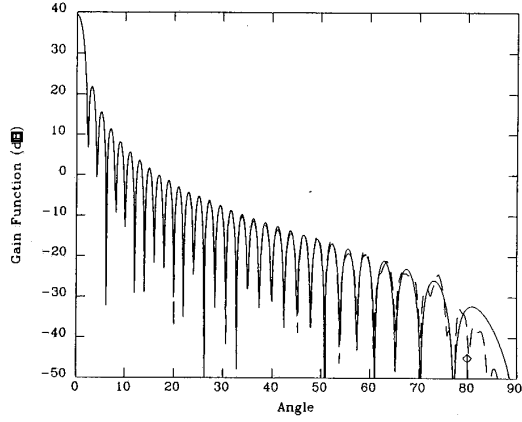


Fig. 5. Gain function of circular-aperture antenna; — exact, --- computed from direct summation.

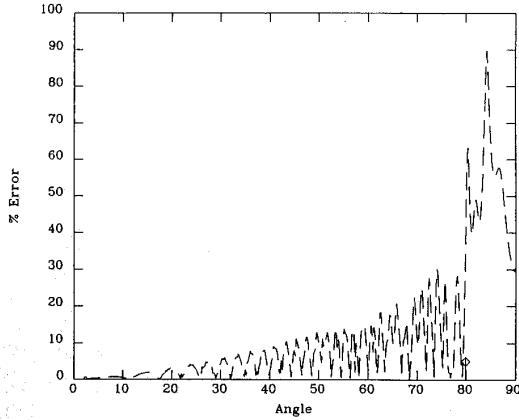


Fig. 6. Error between exact and computed far fields of Fig. 5.

assumed bandwidth of $k^+ = k$ for $\lambda/2$ near-field sample spacing is an extremely good approximation. However, (44) and (39) apply exactly to bandlimited functions only for an infinite near-field scan plane. Since our scan plane is truncated at $\rho = \rho_0$, errors are introduced into the far-field pattern that increase as the angle from boresight approaches the scan limit angle [26]. As the radius of the scan plane gets larger, the errors in using the reconstruction-sampling equations approach zero. Whereas, the errors in using the direct sum remain regardless of the radius of the scan plane.

A. Computer Time

The central processing unit (CPU) time to reconstruct the near-field data in (44) and to compute $\bar{D}_0(K)$ in (39) is proportional to $(ka)^2$. For a general (nonsuper-reactive) antenna that does not possess the circular symmetry of our hypothetical aperture antenna, $\bar{D}_n(K)$ may have to be evaluated for $|n|$ as large as ka . Thus, the total CPU time for processing near-field scanning data in plane-polar coordinates is, in general, proportional to $(ka)^3$. A graph of CPU time, on a one MFLOP linpack-performance-rated computer, versus the electrical size of the antenna for plane-polar scanning may be found in [17, fig. 11].

The CPU times for plane-polar computations may be reduced by evaluating indirectly the radial integrals in (30) with the help of "fast Hankel transforms" [27], [28]. These methods either require unequal radial sample spacing [27], [2] or encounter numerical difficulties for large n [28], [6]. More importantly, however, none of these fast Hankel transform methods for evaluating the radial integrals is based on a rigorous sampling theorem. Convergence of the summations must be determined by choosing successively smaller sample spacings that are generally much smaller than $\lambda/2$ before accurate convergence is reached [2], [6].

Of course, a viable alternative for reducing computer processing time is to approximately interpolate the near-field data taken on a plane-polar lattice to obtain near-field data on a rectangular lattice with $\lambda/2$ spacings in x and y [22], [29]–[31], [8]. (By singling out the far-field propagation exponential, Bucci *et al.* [8] also derive an approximate method for increasing the measured data-point spacing beyond $\lambda/2$ for scan plane distances z_0 greater than the radius of the test antenna.) If one can tolerate the errors introduced by the approximate interpolation procedure (rigorous interpolation from (ρ, ϕ) to (x, y) points through reconstruction takes a CPU time proportional to between $(ka)^3$ and $(ka)^4$), the interpolated plane-rectangular data can be summed to get the full far field in a CPU time proportional to $(ka)^2 \log ka$ [17].

APPENDIX

PROOF THAT THE PROBE RESPONSE OBEYS THE HOMOGENEOUS SCALAR WAVE EQUATION

From [11, pp. 87 and 121] or [9, eq. (1)] the output of the probe can be written as

$$b_p(\bar{r}) = \frac{a_0}{1 - \Gamma_L \Gamma_0} \int_{-\infty}^{\infty} \int_{-\infty}^{\infty} \bar{s}'(\bar{K}) \cdot \bar{s}(\bar{K}) e^{i\bar{k} \cdot \bar{r}} d\bar{K} \quad (\bar{k} = \bar{K} + \gamma \hat{z}) \quad (48)$$

where $\bar{s}(\bar{K})$ and $\bar{s}'(\bar{K})$ are the vector transmitting and receiving plane-wave spectra of the test and probe antennas, respectively. The plane-wave "transmission formula" (48) assumes that the probe translates without rotation with respect to the test antenna, and neglects multiple interactions between the test and probe antennas. It holds in the positive z half space, $z > d$, where d is the minimum value of z outside of which the test and probe antennas do not intersect for all x and y .

Taking the Laplacian ∇^2 of (48) and interchanging the differentiation and integration, one finds

$$\nabla^2 b_p(\bar{r}) = \frac{a_0}{1 - \Gamma_L \Gamma_0} \int_{-\infty}^{\infty} \int_{-\infty}^{\infty} \bar{s}'(\bar{K}) \cdot \bar{s}(\bar{K}) \nabla^2 (e^{i\bar{k} \cdot \bar{r}}) d\bar{K}. \quad (49)$$

Because

$$\nabla^2 (e^{i\bar{k} \cdot \bar{r}}) = -k^2 e^{i\bar{k} \cdot \bar{r}} \quad (50)$$

the right-hand side of (49) equals $-k^2$ times the right-hand side of (48). Thus (49) can be written

$$\nabla^2 b_p(\bar{r}) + k^2 b_p(\bar{r}) = 0. \quad (51)$$

Q.E.D.

Because the integrand in (48) decays exponentially for $K > k$, the interchange of the Laplacian differentiations and the infinite-limit integrations in (49) are proven rigorously valid by the theorems found in a number of textbooks; for example, Kaplan [32, sec. 6-23] or Bochner and Chandrasekharan [33, theorem 62]. (The exponential decay of the integrand in (48) makes the limits of integration virtually finite. Thus, one would indeed expect from Leibnitz's rule for finite integrals [32, sec. 4-12] that the interchange of differentiations and integrations is permissible.)

At first sight, one may think that (51) holds only in the half-space $z > d$, which indeed is the region of concern for plane-polar scanning. However, (48) holds for an arbitrarily directed z -axis, and therefore $b_p(\vec{r})$ satisfying (51) is uniquely defined in all the overlapping parts of the half-space regions determined by the different z -axes, provided, of course, that the probe translates without rotation with respect to the test antenna, and multiple interactions are negligible. In other words, (48) uniquely defines $b_p(\vec{r})$ satisfying (51) for all points in space where (48) is a valid expression, in particular, for r greater than the sum of the radii of the test and probe antennas [9].

ACKNOWLEDGMENT

Carl F. Stubenrauch and Ronald C. Wittmann of the National Institute of Standards and Technology contributed useful recommendations for revising the original manuscript. Helpful technical comments were also contributed by an anonymous reviewer. Margaret B. Woodworth wrote the computer programs.

REFERENCES

- [1] Y. Rahmat-Samii, V. Galindo-Israel, and R. Mittra, "A plane-polar approach for far-field construction from near-field measurements," *IEEE Trans. Antennas Propagat.*, vol. AP-28, pp. 216-230, 1980.
- [2] C. F. Stubenrauch, "Planar near field scanning in polar coordinates: A feasibility study," Nat. Bur. Stand. Rep. SR-723-73-80, Boulder, CO, 1980.
- [3] M. Israel and B. Cyzys, "Probe compensation for planar polar near field measurements without probe rotation," in *IEEE Antennas Propagat. Soc. Dig. Symp.*, Houston, TX, 1983, pp. 557-560.
- [4] P. F. Wacker and R. Severyns, "Near field analysis and measurement: plane polar scanning," *Inst. Elec. Eng. Conf. Pub.* 219, pt. 1, pp. 105-107, 1983.
- [5] Y. Rahmat-Samii and M. S. Gatti, "Far-field patterns of spaceborne antennas from plane-polar near-field measurements," *IEEE Trans. Antennas Propagat.*, vol. AP-33, pp. 638-648, 1985.
- [6] C. Cao, E. Van Lil, A. Van de Capelle, and K. Van't Klooster, "A comparison of plane-polar near-field to far-field transformation techniques," in *Proc. 11th ESTEC Antenna Workshop*, Gothenburg, Sweden, 1988, pp. 191-195.
- [7] J. C. Bennett and K. S. Farhat, "Near-field measurements on plane-polar facility," *Inst. Elec. Eng. Proc.*, vol. 136, pt. H, no. 3, pp. 202-208, 1989.
- [8] O. M. Bucci, C. Gennarelli, and C. Savarese, "Fast and accurate near-field-far-field transformation by sampling interpolation of plane-polar measurements," *IEEE Trans. Antennas Propagat.*, vol. 39, pp. 48-55, 1991.
- [9] A. D. Yaghjian, "Efficient computation of antenna coupling and fields within the near-field region," *IEEE Trans. Antennas Propagat.*, vol. AP-30, pp. 113-128, 1982.
- [10] J. A. Stratton, *Electromagnetic Theory*. New York, McGraw-Hill, 1941, sec. 6.9.
- [11] D. M. Kerns, "Plane-wave scattering-matrix theory of antennas and antenna-antenna interactions," Nat. Bur. Stand. Monograph 162, U.S. Government Printing Office, Washington, DC, 1981.
- [12] F. H. Larsen and J. E. Hansen, "A dual-polarized probe system for near-field measurements," in *IEEE Antennas Propagat. Soc. Dig. Symp.*, Seattle, WA, 1979, pp. 557-560.
- [13] A. D. Yaghjian and R. C. Wittmann, "The receiving antenna as a linear differential operator: application to spherical near-field scanning," *IEEE Trans. Antennas Propagat.*, vol. AP-33, pp. 1175-1185, 1985.
- [14] P. F. Wacker, "Near-field antenna measurements using a spherical scan: efficient data reduction with probe correction," *Inst. Elec. Eng. Conf. Pub.* 113, pp. 286-288, 1974.
- [15] J. E. Hansen, *Spherical Near-Field Antenna Measurements*. London, U.K.: Peregrinus, 1988.
- [16] A. D. Yaghjian, "Approximate formulas for the far field and gain of open-ended rectangular waveguide," *IEEE Trans. Antennas Propagat.*, vol. AP-32, pp. 378-384, 1984.
- [17] —, "An overview of near-field antenna measurements," *IEEE Trans. Antennas Propagat.*, vol. AP-34, pp. 30-45, 1986.
- [18] A. V. Oppenheim and R. W. Schaffer, *Digital Signal Processing*. Englewood Cliffs, NJ, Prentice-Hall, 1975, ch. 3.
- [19] A. D. Yaghjian, "Near-field antenna measurements on a cylindrical surface: A source scattering-matrix approach," Nat. Bur. Stand., Boulder, CO, Tech. Note 696, 1977.
- [20] G. N. Watson, *Theory of Bessel Functions*, 2nd ed. London, U.K.: Cambridge Univ. Press, 1952, ch. 18.
- [21] R. Barakat, "Application of the sampling theorem to optical diffraction theory," *J. Opt. Soc. Amer.*, vol. 54, no. 7, pp. 920-930, 1964.
- [22] H. Stark, "Sampling theorems in polar coordinates," *J. Opt. Soc. Amer.*, vol. 69, no. 11, pp. 1519-1525, 1979.
- [23] R. C. Wittmann and A. D. Yaghjian, "Spherical-wave expansions of piston-radiator fields," *J. Acoust. Soc. Amer.*, vol. 90, no. 3, pp. 1647-1655, 1991.
- [24] M. Abramowitz and I. A. Stegun, "Handbook of mathematical functions," Nat. Bur. Stand. Applied Math Series 55, U.S. Government Printing Office, Washington, DC, 1964, ch. 9.
- [25] C. C. Johnson, *Field and Wave Electrodynamics*. New York, McGraw-Hill, 1965, sec. 10.5.
- [26] A. D. Yaghjian, "Upper-bound errors in far-field antenna parameters determined from planar near-field measurements, Part 1: Analysis," Nat. Bur. Stand. Tech. Note 667, Boulder, CO, 1975.
- [27] A. E. Siegman, "Quasi fast Hankel transform," *Opt. Lett.*, vol. 1, no. 1, pp. 13-15, 1977.
- [28] E. W. Hansen, "Fast Hankel transform algorithm," *IEEE Trans. Acoust., Speech, Signal Processing*, vol. ASSP-33, pp. 666-671, 1985.
- [29] I. Shenberg and A. Macovski, "A direct MRI Hankel transform system using rotating gradients," *IEEE Trans. Med. Imaging*, vol. MI-5, pp. 121-127, 1986.
- [30] M. S. Gatti and Y. Rahmat-Samii, "FFT applications to plane-polar near-field antenna measurements," *IEEE Trans. Antennas Propagat.*, vol. 36, pp. 781-791, 1988.
- [31] E. Van Lil, C. Cao, A. Van de Capelle, K. Van't Klooster, "A fast interpolation procedure for plane-polar near-field to far-field transforms," in *IEEE Antennas Propagat. Soc. Symp., Dig.*, Dallas, TX, 1990, pp. 244-247.
- [32] W. Kaplan, *Advanced Calculus*. Reading, MA: Addison-Wesley, 1952.
- [33] S. Bochner and K. Chandrasekharan, *Fourier Transforms*. London, U.K.: Princeton Univ. Press, 1949.



Arthur D. Yaghjian (S'68-M'69-SM'84) was born in Providence, RI, on January 1, 1943. He received the B.S., M.S., and Ph.D. degrees in electrical engineering from Brown University, Providence, RI, in 1964, 1966, and 1969.

After teaching mathematics and physics for a year at Hampton Institute, VA, he joined the Electromagnetics Division of the National Bureau of Standards, Boulder, CO. In 1983 he transferred to the Electromagnetic Sciences Division at Hanscom AFB, MA. His major research has been in near-field antenna measurements, electromagnetic theory, and scattering.

Dr. Yaghjian is a member of the IEEE Antennas and Propagation Society, the Electromagnetics Society, the International Union of Radio Science, and Sigma Xi.